JVI
Journals.ASM.org

Infection of Vascular Endothelial Cells with Human Cytomegalovirus under Fluid Shear Stress Reveals Preferential Entry and Spread of Virus in Flow Conditions Simulating Atheroprone Regions of the Artery

Jenny B. DuRose,[a] Julie Li,[b,c] Shu Chien,[b,c] and Deborah H. Spector[a,d]

Departments of Cellular and Molecular Medicine[a] and Bioengineering,[b] Institute of Engineering in Medicine,[c] and School of Pharmacy and Pharmaceutical Sciences, University of California, San Diego, La Jolla, California, USA[d]

Atherosclerosis is a major pathogenic factor in cardiovascular diseases, which are the leading cause of mortality in developed countries. While risk factors for atherosclerosis tend to be systemic, the distribution of atherosclerotic plaques within the vasculature is preferentially located at branch points and curves where blood flow is disturbed and shear stress is low. It is now widely accepted that hemodynamic factors can modulate endothelial gene expression and function and influence the pathophysiological changes associated with atherosclerosis. Human cytomegalovirus (HCMV), a ubiquitous pathogen, has long been proposed as a risk factor for atherosclerosis. To date, the role of HCMV in atherogenesis has been explored only in static conditions, and it is not known how HCMV infection is influenced by the physiological context of flow. In this study, we utilized a parallel-plate flow system to simulate the effects of shear stresses in different regions of the vasculature *in vitro*. We found that endothelial cells cultured under low shear stress, which simulates the flow condition of atheroprone regions *in vivo*, are more permissive to HCMV infection than cells experiencing high shear stress or static conditions. Cells exposed to low shear stress show increased entry of HCMV compared to cells exposed to high shear stress or static conditions. Viral structural gene expression, viral titers, and viral spread are also enhanced in endothelial cells exposed to low shear stress. These results suggest that hemodynamic factors modulate HCMV infection of endothelial cells, thus providing new insights into the induction/acceleration of atherosclerosis by HCMV.

Cardiovascular diseases represent the leading cause of death in industrialized nations. Atherosclerosis is understood to be the major underlying cause of cardiovascular diseases, particularly in myocardial infarction and stroke. Atherosclerosis is widely recognized as an inflammatory disorder characterized by endothelial dysfunction, increased smooth muscle cell proliferation, and infiltration of macrophages and lymphocytes into the artery wall (18, 25, 32, 35). Identification of the pathophysiological events that occur to induce and maintain these inflammatory and proliferative responses will be critical for treatment and ultimately prevention of cardiovascular disease. Since the 1970s, there has been increasing interest in the possible role of viral infection in the pathogenesis of atherosclerosis.

Human cytomegalovirus (HCMV) is a widely disseminated pathogen that establishes a lifelong persistent infection and is typically asymptomatic in the immunocompetent host (29). HCMV infection can cause life-threatening complications in immunocompromised individuals and is the leading viral cause of birth defects. Transmission of HCMV can occur during gestation or throughout life by direct contact with infected bodily fluids. In the United States, the seroprevalence of HCMV in children age 6 to 11 is 37% and then gradually increases to nearly 100% by the ninth decade of life (2).

While HCMV infection has traditionally been thought of as inconsequential to the immunocompetent host, its potential involvement in cardiovascular disease highlights the need for further investigation. Cells that are important for atherosclerosis, including vascular endothelial cells, smooth muscle cells, and monocyte/macrophages, are targets of HCMV infection *in vivo* (19, 21, 27). Based on results from *in vitro* studies, HCMV has been proposed to be involved in the pathogenesis of atherosclerosis, possibly by the activation of inflammatory pathways (3, 15) or by promoting the migration and proliferation of smooth muscle cells (33, 41). This has been supported by work in rodent models, which have shown that infection with CMV increased aortic expression of proatherosclerotic genes and lesion size (8, 22), leukocyte infiltration (45), and intimal thickening (9, 24).

A strong support for the causative link between HCMV infection in atherosclerosis in humans has been provided by studies following organ transplantation, and antiviral therapies have proven to be effective at improving allograft survival in transplant patients (28, 43). The link between HCMV infection and induction and/or promotion of atherosclerosis in immunocompetent individuals has been more controversial, in part due to apparent contradictions in clinical data. One particular complication in the interpretation of clinical data is that the age at which the individual acquired HCMV infection is typically unknown. Like HCMV infection, atherosclerosis increases with age, and the extent by which HCMV promotes atherosclerosis may differ depending on the health of the vascular system at the time of infection or simply

Received 20 August 2012 **Accepted** 3 October 2012
Published ahead of print 10 October 2012
Address correspondence to Deborah H. Spector, dspector@ucsd.edu.

doi:10.1128/JVI.02244-12

the amount of time HCMV is present within the vascular system. Some clinical studies have reported that atherosclerotic and healthy individuals have equal association of HCMV genomes in the vascular system as well as seropositivity (21, 34). However, when the severity of infection, viral gene expression, and/or antibody titer are taken into account, it has been reported that there is a very strong association between HCMV infection and atherosclerosis (1, 5, 26, 31, 49). These findings suggest that simple exposure to HCMV does not put one at risk for cardiovascular disease, but rather having a high level of HCMV disease and/or a robust immunological response increases the risk of developing atherosclerosis.

In healthy blood vessels, the endothelium acts as a physical barrier in addition to performing functions that maintain vessel homeostasis. In general, risk factors that promote atherogenesis are systemic, while atherosclerotic lesions occur principally in large- and medium-sized arteries in regions that are exposed to disturbed blood flow and low wall shear stress. Interaction between hemodynamic forces and the endothelium has emerged as a critical regulator of normal cardiovascular function, development, and pathology (11). Surprisingly, the role of blood flow patterns and fluid shear stress has never been studied in the context of infection with HCMV or even with other blood-borne viruses. Like other risk factors, it is possible that HCMV infection promotes atherosclerotic lesions only in atheroprone regions of the vascular system.

Given the prevalence of HCMV in the human population and the mortality associated with atherosclerosis, there is a great need to understand the bidirectional interactions of HCMV and the endothelium in the physiological and pathophysiological conditions that occur in the human artery. To our knowledge, the studies presented here are the first to address this question. Utilizing a parallel-plate flow chamber, we have investigated the effects of variation in shear stress on HCMV infection of primary endothelial cells *in vitro*. We have found that exposure of endothelial cells to low shear stress enhances the dynamics of HCMV infection from entry to viral gene expression and spread. Our results suggest that endothelium located in the low-shear atheroprone regions has increased permissivity to HCMV infection. If HCMV infection can act to promote atherosclerotic lesions, its predilection for atheroprone regions of the vascular system may have a significant impact on the pathogenesis of atherosclerosis.

MATERIALS AND METHODS

Cells and viruses. Human aortic endothelial cells (ECs) were purchased from Cell Applications. Human foreskin fibroblasts (HFFs) were obtained from the Medical Center of the University of California, San Diego. The endotheliotropic HCMV strain TB40/E was a gift from Christian Sinzger, Eberhard-Karls-Universität, Tübingen, Germany. An additional clinical isolate from a deidentified patient was obtained from the Medical Center of the University of California, San Diego. To produce high-titer stocks, infectious supernatants from ECs were passaged a single time on HFFs. Supernatants from viral or mock infections were centrifuged at 1,000 × *g* to remove cells and debris. The titers of cell-free supernatants were determined by plaque assay on HFFs, and endothelial tropism was confirmed by immunofluorescence in ECs.

Tissue culture. ECs were cultured in 25% endothelial cell growth medium (ECGM; Cell Applications) and 75% M199 medium (Mediatech) supplemented with 20% inactivated fetal bovine serum (FBS), 2 mM L-glutamine, 1 mM sodium pyruvate, 100 U/ml penicillin, 100 μg/ml streptomycin, and 1.5 μg/ml amphotericin B. HFFs were cultured in minimal essential medium (MEM; Gibco) supplemented with 10% FBS, 1.5 μg/ml amphotericin B, 2 mM L-glutamine, 100 U/ml penicillin, and 100 μg/ml streptomycin. Cells were incubated at 37°C with 5% CO_2 for ECs or 7% CO_2 for HFFs. During infection, heparin-containing ECGM was removed from the EC medium.

Flow system and chambers. EC monolayers on gluteraldehyde-fixed gelatin-coated glass slides were cultured in parallel-plate flow chambers (17). The flow rate through the channel was regulated by a peristaltic pump equipped with a syringe damper. The flow rate (32 ml/min), channel width (2.5 cm), and length (5 cm) were kept constant, while the channel height was varied by using silicone gaskets of different thicknesses (0.25, 0.5, and 1 mm) to impose different shear stresses (14, 3.5, and 0.9 dyn/cm^2, respectively). The system was kept in a constant-temperature hood at 37°C, and the recirculating medium was ventilated with humidified 5% CO_2-95% air. ECs were exposed to flow for the indicated times (mostly 24 h) and then infected by replacing the medium reservoir with virus-containing medium. After circulating through the system for 6 h, the virus-containing medium was collected and replaced by fresh medium.

Immunofluorescence. EC monolayers on glass slides were washed with phosphate-buffered saline (PBS), fixed 15 min with 2% formaldehyde in PBS, and permeabilized 5 min with 0.2% Triton X-100 in PBS. Cells were blocked with 10% normal goat serum in PBS, incubated with primary antibodies against IE1/IE2 (clone CH160), UL99 (clone CH19), and UL83 (clone CH12) purchased from Virusys, and then incubated with isotype-specific tetramethyl rhodamine isocyanate (TRITC)- or fluorescein isothiocyanate (FITC)-conjugated secondary antibodies (Southern Biotech) with Hoescht 33342 (Calbiochem) to stain nuclei. Coverslips were mounted on slides with Prolong gold antifade (Invitrogen). No staining was observed in mock-infected cells.

Entry assay. ECs were exposed to flow for 24 h and infected with TB40/E (3 PFU/cell) for the indicated times. Cells were washed with ice-cold PBS to remove unbound virus. For total virus, cells were collected with a cell scraper. For internalized virus, cells were incubated 1 min with ice-cold 40 mM sodium citrate (pH 3) in PBS to inactivate adsorbed virus. Control cells were incubated on ice for 1 h prior to infection and maintained on ice until after virus inactivation. Cells were then trypsinized, quenched in medium, washed with PBS, and then incubated 5 min with pronase E (0.5 mg/ml, Calbiochem) in PBS. Following pronase treatment, cells were quenched in medium and washed extensively with PBS.

Quantitative PCR. Cellular and viral genomic DNA was isolated from ECs with the QiaAmp DNA blood minikit (Qiagen). Cellular RNA was isolated from ECs using TRIzol (Invitrogen) according to the manufacturer's instructions. Purified RNA was treated with RQ1 DNase (Promega) to remove contaminating genomic DNA. Reverse transcription was performed on 1 μg of RNA per sample using Thermoscript reverse transcriptase (Invitrogen). To detect viral DNA, quantitative PCR (qPCR) analysis was performed in an Applied Biosystems ABI Prism 7700 sequence detection system with 50 ng of genomic DNA per reaction using TaqMan universal PCR master mix (Applied Biosystems). Primers and TaqMan dually labeled probes (5′-6-carboxyfluorescein [FAM] and 3′-black hole quencher) were directed against the GAPDH promoter for cellular DNA and the unspliced UL77 gene for viral DNA. Viral DNA was normalized to cellular genomic DNA. To analyze viral mRNA expression, qPCR was performed as stated above with either TaqMan universal PCR master mix or Power SYBR PCR master mix (for UL32, UL55, and tubulin). Expression levels of viral genes were normalized to cellular α-tubulin. See Table 1 for PCR primers and probes.

Western blotting. ECs were lysed in Triton lysis buffer containing 50 mM Tris-HCl (pH 8.0), 150 mM NaCl, 1% Triton X-100, 1 mM EDTA (pH 8.0), 50 mM NaF, 1 mM $NaVO_4$, 10 mM Na pyrophosphate, 10 mM β-glycerophosphate, 100 mM phenylmethylsulfonyl fluoride (PMSF), and 1× protease inhibitor cocktail (Sigma). Lysates were sonicated to shear genomic DNA, quantified by Bradford assay, run on 8 or 10% polyacrylamide gels, and transferred to nitrocellulose membranes. Mem-

TABLE 1 Primers and probes for quantitative real-time quantitative PCR and RT-PCR

Transcript	Forward primer	Reverse primer	Probe[a]
IE2 86	TGACCGAGGATTGCAACGA	CGGCATGATTGACAGCCTG	TGGCAGAACTCGGTGACATCCTCGCC
IE2 exon 5	GCGCAATATCATGAAAGATAAGAAC	GATTGGTGTTGCGAAACATG	TCGGCGGGGTGGC
UL32	GGTTTCTGGCTCGTGGATGTCG	CACACAACACCGTCGTCCGATTAC	SYBR green
UL55	AGCTGCGTGACCATCAACCAAACC	CTGCGAGTAAAGTTCCAGTACCC	SYBR green
UL77	CGTTGCCCGGGAACG	GGTGTGAAAGCGGATAAAGGG	ACCTAGCTACTTTGGAATCACGCAGAACGA
UL83	TCTTCCTGGAGGTACAAGCCA	CAGCCACGGGATCGTACTG	ACGCGAGACCGTGGAACTGCG
UL84	AGACATTGGGACCCTCCGTC	GCGGTGATTCGTTCGGG	TGGACGATTGGAGCTAG
α-Tubulin	AGATGCCAAGTGACAAGACC	TCCAACACAAGGTCAATGATCTC	SYBR green
GAPDH promoter	TTTCATCCAAGCGTGTAAGGG	CAGGACTGGACTGTGGGCA	CCCCGTCCTTGACTCCCTAGTGTC

[a] All TaqMan probes have a 5′ 6-carboxyfluorescein (FAM) and 3′ black hole quencher (BHQ) modification.

branes were probed with the following antibodies: IE1/2 (clone CH160), UL44 (clone CH13), UL55 (clone 2F12), UL57 (clone CH167), UL83 (clone CH12), UL84 (clone MAb84), UL99 (clone CH19), all purchased from Virusys; IE1/2 (clone 8140; Chemicon); α-tubulin (clone DM 1A; Sigma-Aldrich); and UL32, UL85, and UL86 (gifts from Bill Britt).

Analysis of cell-associated and released virus. For cell-associated virus, glass slides were collected at 96 h postinfection (p.i.), washed with PBS, trypsinized, quenched in medium, and centrifuged at 500 × *g* for 4.5 min. Cell pellets were washed in PBS and then snap-frozen in liquid N_2 and stored at −80°C. Cell pellets were resuspended in ice-cold HFF medium and sonicated for a total of 3 min on ice with a Misonix Sonicator 3000 at power level 10 using a cup horn attachment. Complete cell lysis was evaluated by staining cell sonicate with trypan blue. For released virus, medium was collected at 48 and 96 h p.i. and centrifuged at 500 × *g* for 4.5 min to remove cell debris. Cell-free supernatant was removed and dimethyl sulfoxide (DMSO) was added to a final concentration of 1% before freezing and storing at −80°C. The titer of cell-associated and released virus was determined on HFFs by plaque assay.

Transmission electron microscopy. After 96 h p.i., glass slides were placed directly into 2% glutaraldehyde and 0.1 M cacodylate buffer (pH 7.4) for 2 min at room temperature, followed by 4°C for at least 4 h. Cell pellets were postfixed in 1% osmium tetroxide in 0.1 M cacodylate buffer for 1 h on ice, stained *en bloc* in 2% uranyl acetate for 1 to 2 h on ice, dehydrated in ethanol on ice, embedded in epoxy resin, sectioned at 60 nm, and collected onto 200 mesh copper grids. Grids were viewed using a JEOL 1200EX II transmission electron microscope and photographed using a Gatan digital camera.

Statistical analysis. Data represent means ± standard deviations (SD) of a minimum of three independent experiments. Significance was determined by analysis of variance (ANOVA) with Tukey-Kramer's *post hoc* test.

RESULTS

Exposure to low shear stress enhances entry of HCMV into endothelial cells. To investigate the effect of shear stress on HCMV entry, primary human aortic endothelial cells (ECs) were exposed to three levels of laminar shear stress in parallel-plate flow chambers prior to infection with HCMV endotheliotropic strain TB40/E at a multiplicity of 3 PFU per cell. The three levels of shear stress were generated by keeping flow rate and channel width constant while varying the channel height. Cells were exposed to static conditions (STAT; 0 dyn/cm^2), low shear stress (LSS; 0.9 dyn/cm^2), moderate shear stress (MSS; 3.5 dyn/cm^2), and high shear stress (HSS; 14 dyn/cm^2) for 24 h prior to infection to allow cells to acclimate to flow conditions. During the 6 h of infection, the reservoir volume was reduced to 35 ml; thus, the flow rate of 32 ml/min allowed essentially the entire medium reservoir volume to recirculate through each channel every minute. Cells maintained in STAT were infected at the same multiplicity in an equivalent volume as cells exposed to shear stress. At 6 h postinfection (p.i.), the virus-containing medium was replaced with fresh medium. Infected ECs were analyzed by immunofluorescence assay (IFA) for expression of immediate-early (IE) proteins at 24 h p.i. (Fig. 1A). There was no statistically significant difference in the percentage of IE-positive cells (IE+) when exposed to STAT or HSS ($P > 0.05$), while cells exposed to MSS and LSS had increasing percentages of IE+ cells (Fig. 1B). This shear-stress-dependent variation in IE expression was not unique to TB40/E, as we obtained similar results with another HCMV clinical isolate (Fig. 1C).

One possible explanation for the reduced number of IE+ cells in ECs exposed to increasing shear could be that the increased friction on the cell surface interfered with HCMV adsorption. Alternatively, it was also possible that cellular adaptation to shear stress altered permissivity to HCMV entry or IE expression. To test these possibilities, we exposed cells to shear or STAT for 0, 6, or 24 h prior to infection with TB40/E (3 PFU/cell). For this experiment, low-, moderate-, and high-shear chambers were run in the same channel and perfused with the same virus-containing medium. We reasoned that if friction alone damaged the virus or reduced adsorption, we would see a difference in infectivity immediately upon application of shear stress. We found that when ECs were infected concurrently with their exposure to shear stress (Fig. 1D, 0 h), there was no significant difference (NS) in the percentage of IE+ cells ($P = 0.19$) in the different shear conditions. The percentage of IE+ cells increased over time in ECs exposed to MSS and LSS, reaching a maximum at 24 h p.i., while there was no change in infectivity of ECs exposed to HSS or STAT (Fig. 1D). These results suggest that friction alone does not impair HCMV entry, but rather a cellular adaptation to LSS and MSS increases permissivity of ECs to HCMV entry or IE expression.

In order to determine whether HCMV adsorption/penetration or IE expression was affected in ECs exposed to shear stress, we used quantitative PCR (qPCR) to measure the adsorption and internalization of viral genomes. ECs were exposed to LSS or HSS for 24 h and then infected with TB40/E (3 PFU/cell). To isolate internalized viral DNA, cells were trypsinized, treated with protease, and washed extensively to facilitate removal of external virus. For each experiment, control cells were allowed to adsorb virus at 4°C, thus preventing internalization, and protease treatment effectively removed at least 90% of the bound virus from the cell surface (data not shown). When ECs were exposed to virus for 6 h, as in Fig. 1A and B, we found that the amount of internalized viral DNA was comparable to IE expression (Fig. 1E, black bars, and B). The analysis of variance (ANOVA) failed to achieve sta-

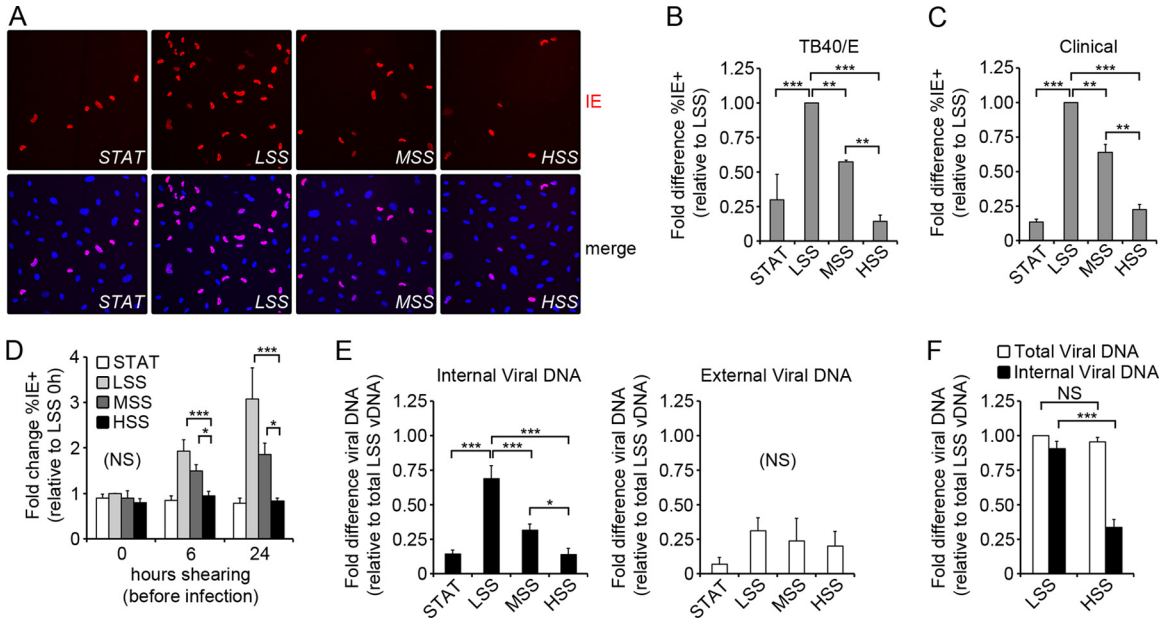

FIG 1 Penetration of HCMV varies inversely with the applied shear stress. (A) ECs were infected with TB40/E (3 PFU/cell) and assayed for IE expression (red) by IFA at 24 h p.i., and nuclei were stained with Hoechst (blue). (B) The fold difference (relative to LSS) in the percentage of IE-positive cells (%IE+) at 24 h p.i., as shown in panel A. The %IE+ was calculated by counting approximately 1,000 cells per condition and averaging the results from 3 independent experiments. For LSS, the percentage of IE+ cells was an average of 59% ± 3%. (C) ECs were infected with an additional HCMV clinical isolate (3 PFU/cell) and assayed for IE expression by IFA at 24 h p.i. Cells were counted as stated for panel A, and the fold difference (relative to LSS) in the %IE+ is shown. For LSS, the percentage of IE+ cells was an average of 44% ± 6%. (D) Cells were infected following exposure to shear stress for the indicated amount of time. Slides were assayed for IE expression at 24 h p.i. by IFA and counted as stated for panel B. The fold change in %IE+ cells is relative to LSS at 0 h for all conditions. For LSS, the percentage of IE+ cells at 0 h p.i. was an average of 26% ± 6%. (E) The fold difference in the abundance of viral DNA (vDNA) at 6 h p.i., measured by qPCR. External vDNA (white bars) was calculated by subtracting the internal vDNA (black bars) from the total vDNA. All values are relative to the total vDNA from ECs exposed to LSS. (F) The fold difference in the abundance of vDNA at 1 h p.i. was measured by qPCR and is relative to LSS total vDNA. All data (B to F) represent the means ± SD from three independent experiments (*, $P < 0.05$; **, $P < 0.01$; ***, $P < 0.001$).

tistical significance ($P = 0.14$) when comparing the amount of external viral genomes after 6 h of incubation with the virus (Fig. 1E, white bars), suggesting that adsorption levels of virus are equivalent under all conditions after 6 h. We then measured total and internal viral DNA content in ECs exposed to LSS and HSS after 1 h p.i, and we found no statistically significant difference ($P > 0.05$) in the total amount of viral DNA associated with cells (Fig. 1F, white bars). This suggests that there is no difference in viral adsorption in ECs exposed to both LSS and HSS after 1 h. However, ECs exposed to LSS internalized nearly 3-fold more viral genomes than HSS ($P < 0.001$) over the first hour of exposure to the virus, suggesting that viral penetration is much more efficient in ECs in LSS (Fig. 1F, black bars). Taken together, these results suggest that ECs exposed to varied shear stress have an equal propensity to adsorb HCMV virions, while ECs adapted to low and moderate shear stress have an increased permissivity to viral penetration.

Early phases of viral gene expression and viral DNA replication are comparable under HSS and LSS. After the virus enters a permissive cell, HCMV gene expression proceeds in a highly regulated fashion. The first genes expressed are the IE genes, which promote transcription of early genes and prime the host cell for viral replication. In order to investigate whether shear stress influences the HCMV replicative cycle, we reduced the amount of input virus in the LSS channel so that the percentages of initially infected cells (%IE+ by IFA) at 24 h p.i. were equal among STAT, LSS, and HSS. ECs were infected 24 h after exposure to STAT, LSS, and HSS with TB40/E (3 PFU/cell for STAT and HSS, 0.75 PFU/cell for LSS). Cells were collected at various times p.i., and IE protein expression was analyzed by Western blotting (Fig. 2A). A single transcript from the major IE region is alternatively spliced to produce the major IE proteins IE1 72 and IE2 86, which share coding exons 2 and 3. At late times in the infection, additional unspliced transcripts are produced from exon 5 of IE2, producing IE2 60 and IE2 40 proteins (40). We used two antibodies to detect the IE proteins: one recognizing an N-terminal epitope specific for IE1 72 and IE2 86, and the other recognizing a C-terminal epitope specific for IE2 86, IE2 60, and IE2 40. We found that there was a slight lag in IE protein expression in ECs exposed to LSS early in the infection (Fig. 2A, 24 h p.i.). By 48 h p.i., however, the expression of IE1 and IE2 were comparable among all groups; at 72 h p.i. the level of IE2 40, which is expressed at late times, was enhanced in cells exposed to LSS. We analyzed the levels of IE2 RNA by quantitative reverse transcriptase PCR (RT-PCR) and found that there was no significant difference ($P > 0.05$) in the level of IE2 86-specific RNA at any time point in all three conditions (Fig. 2B). At 72 h p.i., when we performed quantitative RT-PCR specific for IE2 exon 5 (IE2 86, 60, and 40), we found a significant increase in exon 5-containing transcripts in ECs exposed to LSS compared to that in cells exposed to HSS ($P < 0.05$) or STAT ($P < 0.01$) (Fig. 2C). Taken together, these data suggest that LSS enhances the expression of IE2 late transcripts leading to increased expression of IE2 40 and 60 proteins.

In the next phase of the viral replicative cycle, viral early genes

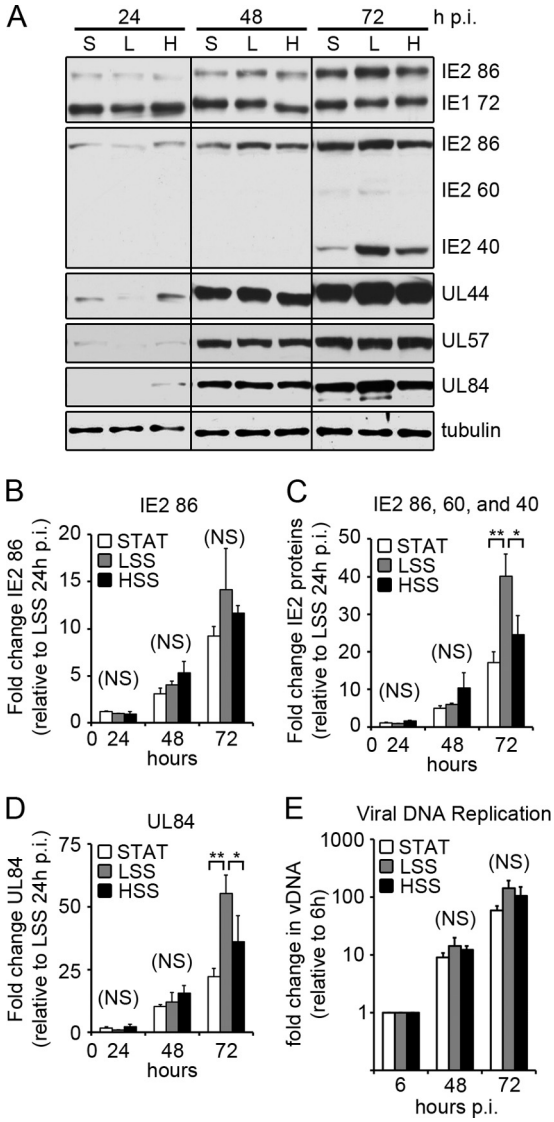

FIG 2 Viral IE and early gene expression. (A) ECs were infected 24 h after exposure to STAT, LSS, and HSS with TB40/E (3 PFU/cell for STAT and HSS; 0.75 PFU for LSS). At the indicated times p.i., cell lysates were assayed for viral protein expression by Western blotting (S, STAT; L, LSS; H, HSS). Here, we show representative blots from five independent experiments. Multiple blots were required to probe for all the proteins. Comparable loading on each blot was confirmed by amido black staining, while one blot was probed for α-tubulin. (B to D) ECs were infected as stated for panel A and collected at the indicated times. Viral mRNA expression was measured by quantitative RT-PCR with primers specific for IE2 86 (B), IE2 exon 5 (C), and UL84 (D). Viral mRNAs were normalized to α-tubulin, and each time point is relative to expression of LSS at 24 h p.i. Data represent the means ± SD from three independent experiments. (E) ECs were collected at the indicated times p.i., and vDNA was measured by qPCR. The fold increase in vDNA was calculated relative to input vDNA (at 6 h p.i.). Data represent means ± SD from 3 independent experiments.

mediate viral DNA replication and act to further subvert host cell function to promote viral replication. We followed the expression of three early genes, the UL44, UL57, and UL84 genes, which are essential for viral DNA replication. Similar to the IE proteins, there was a slight lag in early protein expression in cells exposed to LSS at 24 h p.i. (Fig. 2A). However, by 48 h p.i., early protein expression in cells exposed to LSS is comparable to that of the HSS group, with even slightly higher levels of UL44 and UL84 proteins at 72 h p.i. We analyzed the expression of UL84 mRNA by quantitative RT-PCR and found at 72 h p.i., there was enhanced UL84 mRNA expression in ECs exposed to LSS compared to STAT ($P < 0.01$) and HSS ($P < 0.05$) (Fig. 2D). To determine whether shear stress had an impact on viral DNA replication, cells were infected as stated in the legend to Fig. 2A and collected 6, 48, and 72 h p.i. Viral DNA was isolated and measured by quantitative PCR (Fig. 2E). We found no statistically significant difference in the synthesis of viral DNA at 48 h ($P = 0.30$) or 72 ($P = 0.16$) h p.i., indicating that shear stress has little effect on the early phase of the infection, including viral DNA replication, once the virus has entered the cell.

Late gene expression and spread are enhanced in ECs exposed to LSS. After viral DNA replication, expression of late viral genes (primarily encoding structural proteins) is initiated. To determine if shear stress had an effect on late gene expression, we probed the same lysates as those shown in Fig. 2A for viral late proteins (Fig. 3A). We analyzed the expression of genes in all classes of structural proteins: capsid proteins (UL86 and UL85), tegument proteins (UL83, UL99, UL32), and glycoproteins (UL55). With the exception of UL83, each of these proteins is essential for HCMV replication *in vitro* (38). At 72 h p.i., the expression of all of the late proteins tested increased in ECs exposed to shear stress, with LSS having the highest expression (Fig. 3A). ECs maintained in STAT began to express each of the late proteins by 96 h p.i., while the enhanced expression in ECs exposed to LSS continued to increase. We analyzed the expression of several late viral genes by quantitative RT-PCR to determine if the differences in expression levels were due to a translational effect or were at the mRNA level. Transcript levels of UL32, UL55, and UL83 correlated with protein expression (Fig. 3B to D), suggesting that the increased protein levels were likely due to an increase of the mRNA, possibly through increased transcription.

To further evaluate late viral gene expression in ECs exposed to shear stress, we used IFA to monitor late gene expression at the cellular level. ECs were infected as described in Fig. 2, collected at 24 and 96 h p.i., and each slide was stained with antibodies directed against the N terminus of IE1/IE2, UL99, and UL83. Figure 4A shows representative images of one of four independent experiments. At 24 h p.i., the number of IE+ cells (red) is equivalent among all conditions, averaging 25% ± 5% across all four experiments (Fig. 4A, top). At 96 h p.i., juxtanuclear staining of UL99 protein (green) indicates its appropriate localization to the cytoplasmic viral assembly compartment under each condition, with the number of cells expressing UL99 being significantly higher in ECs exposed to LSS (Fig. 4A, bottom). We counted approximately 1,000 cells per condition for each of 4 independent experiments and found that the number of ECs that expressed UL99 at 96 h p.i. was comparable to the number of ECs that expressed IE proteins at 24 h p.i., suggesting that under LSS, all of the initially infected cells expressed UL99 by 96 h p.i. In contrast, the numbers of ECs exposed to STAT and HSS that expressed UL99 at 96 h p.i. were only 31 and 40%, respectively, of the initially infected cells, suggesting that a large number of cells were significantly delayed or failed to express UL99. In addition to UL99, we analyzed by IFA the expression of UL83, which is a tegument protein that undergoes a nuclear-to-cytoplasmic translocation late in the infection.

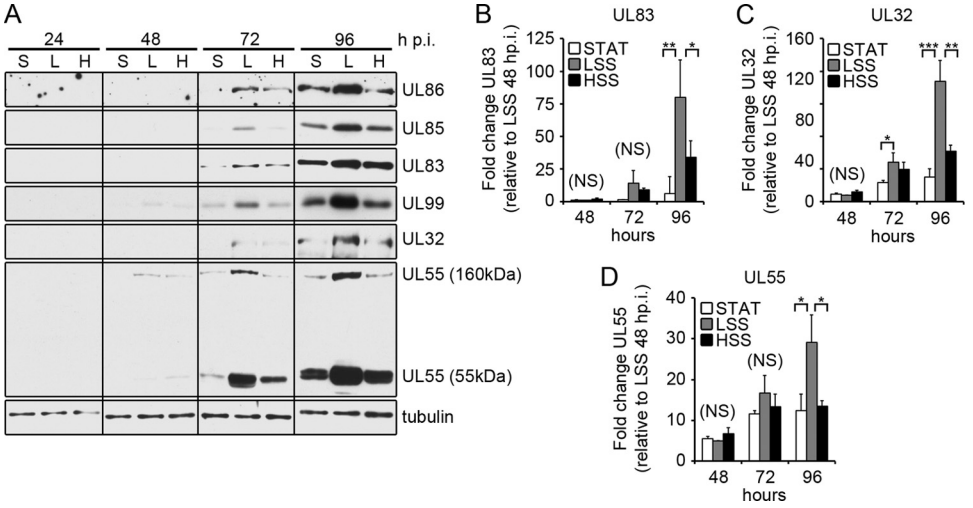

FIG 3 LSS enhances late gene expression. (A) The same lysates as those shown in Fig. 2A were assayed for late viral protein expression by Western blotting. Multiple blots were required to probe for all the proteins, and even loading on each blot was confirmed by amido black staining. One blot for all samples was probed for α-tubulin, as shown in Fig. 2A. (B to D) ECs were infected as stated for Fig. 2A and collected at the indicated times. Viral mRNA expression was measured by quantitative RT-PCR with primers specific for UL83 (B), UL32 (C), and UL55 (D). Viral mRNAs were normalized to α-tubulin, and each time point is relative to expression of LSS at 24 h p.i. Data represent the means ± SD from three independent experiments. (*, $P < 0.05$; **, $P < 0.01$; ***, $P < 0.001$).

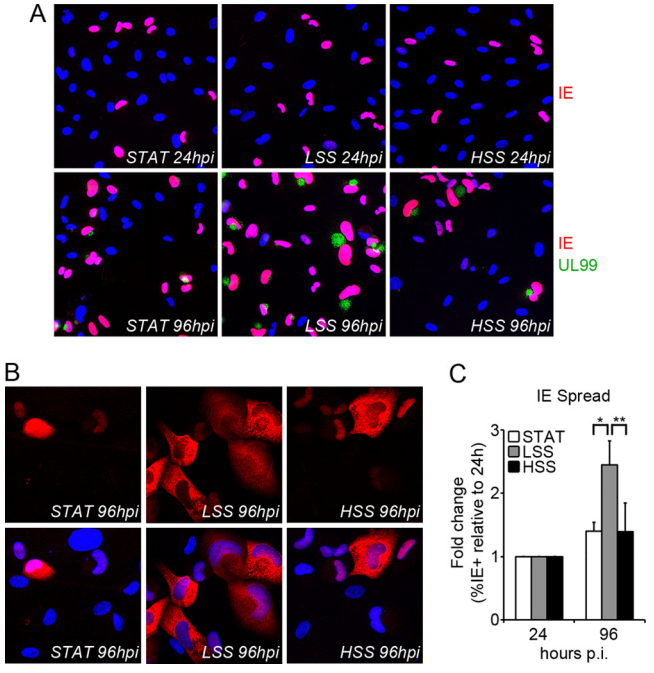

FIG 4 LSS enhances late gene expression and spread of IE expression. (A) ECs were infected with TB40/E as stated for Fig. 2. Slides were collected at the indicated times, and IFA was performed with antibodies directed against IE1/2 (red) and UL99 (green), and nuclei were stained with Hoechst (blue). (B) IFA was performed with antibodies directed against UL83 (red). Nuclei were stained with Hoechst (blue). (C) The fold change in the percentage of IE+ cells relative to initially infected cells (%IE at 24 h). The %IE+ was calculated by counting approximately 1,000 cells per condition and averaging the results from 4 independent experiments. For LSS, the percentage of IE+ cells was 25% ± 5% at 24 h p.i. and increased to 79% ± 9%. (*, $P < 0.05$; **, $P < 0.01$; ***, $P < 0.001$).

We found that UL83 was able to correctly localize to the cytoplasm in all three conditions, but similar to UL99, there were far more ECs with cytoplasmic UL83 when exposed to LSS compared to STAT and HSS (Fig. 4B). When we compared the number of ECs with cytoplasmic UL83 relative to initially infected cells, we found that ECs exposed to LSS expressed significantly more cytoplasmic UL83 than STAT and HSS did ($P < 0.001$). We counted approximately 1,000 cells per condition for each of 4 independent experiments and found that nearly all of the initially infected cells expressed cytoplasmic UL83 in ECs exposed to LSS, while only 16 and 27% of initially infected ECs exposed to STAT and HSS, respectively, expressed UL83 in the cytoplasm. Taken together, these data suggest that after viral DNA replication, the late phase of the infection proceeds at a higher rate in ECs exposed to LSS.

HCMV has a lengthy replicative cycle, and it takes days to produce the first viral progeny. In ECs exposed to shear stress, cell-free virus was detected in the tissue culture medium by 72 h p.i., and cells with small foci of IE proteins in their nuclei were detected by IFA, indicating that spread was starting to occur (data not shown). After 96 h p.i. the percentage of IE+ cells increased in all three conditions, indicating that the infection was able to spread to adjacent cells (Fig. 4A, bottom). In ECs exposed to LSS, the expression of IE proteins spreads throughout the culture at a much higher rate than ECs exposed to STAT and HSS. Plotting of the percentage of IE+ cells at 96 h p.i. relative to the number of initially infected cells (%IE+ at 24 h p.i.) shows a significantly higher rate of spread of HCMV IE proteins in ECs exposed to LSS than that of ECs exposed to HSS ($P < 0.01$) and STAT ($P < 0.05$) (Fig. 4C). The increased late viral gene expression in ECs exposed to LSS (Fig. 3) may have resulted in an overall higher production of viral progeny to lead to increased spread, although the enhanced entry of HCMV into ECs exposed to LSS (Fig. 1) may also be a contributing factor.

LSS enhances production of HCMV infectious progeny. In order to determine whether ECs exposed to LSS produced higher

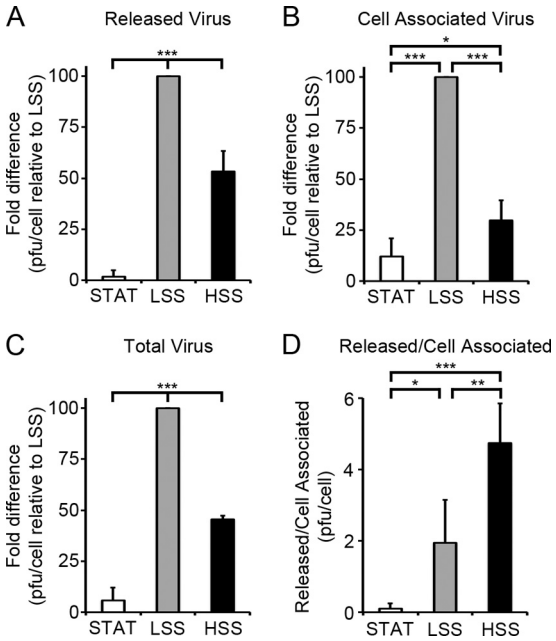

FIG 5 LSS enhances production of infectious viral progeny. ECs were infected with TB40/E as stated for Fig. 2. Slides were collected at 24 h p.i. to determine the number of initially infected cells by IFA against IE proteins. Cell-free supernatants and infected cells were assayed by plaque assay. Cell-free titers at 48 h p.i. were used to determine the number of PFU remaining from the initial infection and subtracted from the titers at 96 h p.i. The PFU/cell was calculated from the number of PFU divided by the number of initially infected cells. For LSS, the total PFU was an average of 1.4 PFU/cell ± 0.4 PFU. Fold difference in the PFU/cell relative to LSS at 96 h p.i. was plotted for released virus (A), cell-associated virus (B), and total virus (C). (D) Ratio of released versus cell-associated virus PFU/cell. Values are means ± SD from at least three independent experiments. (*, $P < 0.05$; **, $P < 0.01$; ***, $P < 0.001$).

titers of virus, we collected cell-free supernatants and infected ECs to analyze the released and cell-associated viral progeny by plaque assay. ECs were infected as described in Fig. 2. Cell-free supernatants and infected ECs were collected at 96 h p.i. in order to analyze the production of viral progeny from a single cycle of infection. The titer of released virus (in PFU/cell) in ECs exposed to LSS was 58-fold greater than that for STAT and 2-fold greater than that for HSS (Fig. 5A). Analysis of the titers of cell-associated virus shows that ECs exposed to LSS produced nearly 8- and 4-fold more PFU/cell than ECs exposed to STAT and HSS, respectively (Fig. 5B). Analysis of the total amount of PFU produced per infected cell indicates that ECs exposed to LSS produced 17- and 2-fold more PFU/cell than ECs exposed to STAT and HSS, respectively (Fig. 5C). ECs exposed to shear stress, regardless of magnitude, released the majority of PFU, while the PFU remained mostly cell associated in ECs exposed to STAT (Fig. 5D). It should be noted that the total PFU released into the medium by ECs exposed to LSS resulted in a concentration of circulating virus in the medium perfusing the cells that was at least 1,000 times lower than the concentration of virus during the initial infection, suggesting that under these conditions, the majority of spread occurred through cell-to-cell transmission rather than through cell-free virus released into the medium. The enhanced late gene expression in ECs exposed to LSS shown in Fig. 3 and 4 may contribute to the overall increased titers in LSS. However, since the levels of the late proteins that were analyzed were comparable in the ECs exposed to HSS and STAT, a global difference in late protein expression is not likely responsible for the 8-fold increase in the total amount of virus produced in ECs exposed to HSS.

Assembly of virions occurs more rapidly in ECs exposed to both LSS and HSS, relative to STAT. One possible explanation for the higher levels of virus produced at 96 h p.i. when ECs were exposed to shear stress was that assembly of the virus particles was more efficient under shear. To address this possibility, we used transmission electron microscopy to visualize the assembly of HCMV virions in the nuclear and cytoplasmic compartments. ECs were infected as stated in Fig. 2, collected at 96 h p.i., and processed for electron microscopy. Electron micrographs of the cytoplasm of ECs exposed to shear stress showed numerous vesicles, dense bodies, intact virions, and noninfectious enveloped particles (NIEPs; Fig. 6A for LSS and 6D for HSS). ECs under STAT conditions contained dense bodies and vesicles. However, greater than 95% of infected cells (Fig. 6G and H) did not contain intact virions or NIEPs. Higher magnifications of the intact virions and NIEPs in the cytoplasm of cells exposed to LSS (Fig. 6B) and HSS (Fig. 6E) clearly show C- and B-type capsids with a surrounding tegument and envelope. Inside the nucleus of infected cells, all three types of capsids are visible, but there are more capsids present in infected ECs exposed to LSS (Fig. 6C) and HSS (Fig. 6F) than in infected ECs exposed to STAT (Fig. 6I). We counted approximately 500 capsids per condition, averaging the results from three independent experiments, and did not see a significant difference ($P = 0.24$) in the percentages of A (9% ± 3%)-, B (76% ± 5%)-, and C (15% ± 3%)-type capsids among STAT, LSS, and HSS, suggesting that capsid assembly and viral DNA packaging occur normally in all three conditions.

To determine if there was a delay in viral assembly and production of infectious virus in ECs exposed to STAT, we analyzed the titers of virus produced and electron micrographs of these cells at 120 h p.i. We found that the released and cell-associated titers increased to within 2-fold of ECs exposed to LSS at 96 h p.i. (data not shown) and that the electron micrographs appeared comparable to ECs exposed to HSS or LSS at 96 h p.i. (Fig. 6J to L). Together, these results suggest that viral assembly occurs more rapidly in ECs exposed to shear stress by approximately 24 h in comparison to ECs under STAT condition.

DISCUSSION

In this report, an *in vitro* parallel-plate flow chamber was used to study the interactions of HCMV and ECs in the physiological context of flow. To our knowledge, this is the first report of EC infection by a blood-borne virus under physiological conditions of flow. Here, we show that exposure of ECs to different magnitudes of laminar shear stress modulates the permissivity to HCMV entry, specifically at the step of viral penetration. LSS, which exists in the atheroprone regions of the arterial tree, enhanced the entry of HCMV in ECs. HCMV entry into the host cell begins with a tethering step to cell surface heparan sulfate proteoglycans (12). Following this initial binding, the virus is thought to engage a cell surface protein receptor, leading to fusion with the cell membrane in fibroblasts (12) or endocytosis in ECs (6). Viral entry into endothelial cells is mediated by the viral envelope glycoprotein complex gH/gL/UL128-131 in a process that requires endocytosis and low-pH-dependent fusion (36, 37). Cell surface proteins that have been proposed to be involved in viral entry include epidermal growth factor receptor (EGFR) (47), platelet-derived growth fac-

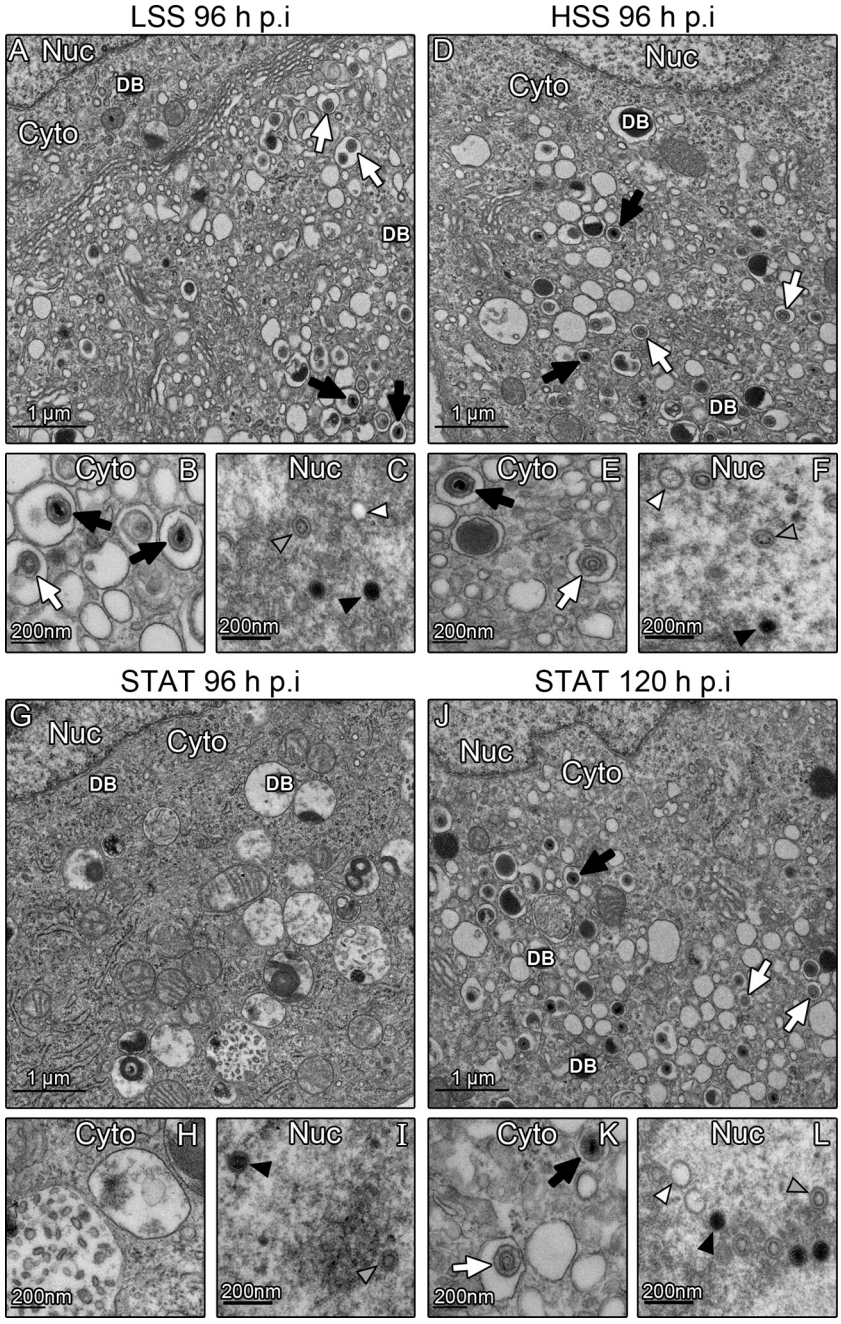

FIG 6 Transmission electron micrographs of infected ECs. ECs were infected with TB40/E as stated for Fig. 2. ECs were fixed for electron microscopy at 96 h p.i. Electron micrographs of infected cell cytoplasm at a magnification of ×2,000 are shown for cells exposed to LSS (A), HSS (D), and STAT (G and J). Nuclei (Nuc), cytoplasm (Cyto), dense bodies (DB), intact virions (black arrows), and noninfectious enveloped particles (white arrows) are indicated. Electron micrographs of infected cell cytoplasm at a magnification of ×10,000 are shown for cells exposed to LSS (B), HSS (E), and STAT (H and L). Electron micrographs of infected cell nuclei at a magnification of ×10,000 for cells exposed to LSS (C), HSS (F), and STAT (I and L). Arrowheads show A capsids (white), B capsids (gray), and C capsids (black).

tor receptor alpha (PDGFRα) (39), and multiple integrins (16, 46). A simple explanation for the increased HCMV penetration into ECs exposed to LSS is that LSS induced expression of one of the potential HCMV receptor proteins. We measured the cell surface expression of heparan sulfate and candidate receptor proteins integrins α2, α6, αvβ3, and β1 both before and after 1 h of exposure to HCMV (data not shown). We found no change in expression upon HCMV exposure; however, we detected a small increase in cell surface heparan sulfate and α6 integrin in cells exposed to HSS. EGFR and PDGFRα have also been implicated in HCMV entry, although we did not detect expression of those proteins in aortic ECs by flow cytometry or Western blotting (data not shown). Another possible explanation for the increased penetration of HCMV in ECs exposed to LSS is that LSS increased the rate

of endocytosis. To determine whether shear stress had an effect on the endocytosis of virus-sized particles, we monitored the endocytosis of 200 nm fluorescently labeled microspheres both before and after 1 h of exposure to HCMV. There was no significant increase in endocytosis of microspheres in ECs exposed to LSS compared to HSS. This suggests that shear stress does not affect the overall rate of fluid-phase endocytosis; however, this may not reflect the rate of receptor-mediated endocytosis of HCMV particles. Taken together, this suggests that the level of expression of these candidate receptors and the rate of general endocytosis are not likely to contribute to increased penetration of HCMV in ECs exposed to LSS. Comparison of the cell surface proteome of ECs in both LSS and HSS and identification of the HCMV receptor will be required in order to further understand the mechanism of enhanced HCMV entry into ECs exposed to atheroprone flow conditions.

While it is well established that atherosclerotic lesions occur preferentially in branch points and curves (areas of LSS), it is currently not known whether HCMV preferentially infects ECs located in atheroprone regions of the arterial tree during acute infection *in vivo*. However, an important clinical study has reported an accumulation of persistently infected ECs in the thoracic aorta adjacent to branch points of the intercostal arteries (31). In this study, *in situ* hybridization and immunohistochemical staining were used to determine the frequency of cells containing the viral genome and of those expressing viral immediate-early gene products in the layers of human aortas with or without visible atherosclerotic lesions. The viral genome could be detected in the majority of both normal (even from young trauma victims) and lesioned vessels, but viral antigen was present only in cells from aortas with lesions. The positive cells were in the endothelial layer lining the lumen and in clusters in the intima/media area adjacent to artery branch points (atheroprone areas of disturbed flow and low shear stress). Interestingly, HCMV antigen was expressed predominantly in lesioned vessels, and in these vessels the HCMV antigen expression was primarily localized to fatty streaks and early atherosclerotic lesions rather than advanced plaques (31). These results suggest that HCMV gene expression may be associated with early events in the pathogenesis of atherosclerosis. Taken together, these data support the hypothesis that direct infection of ECs in atheroprone areas is associated with early atherosclerotic events and may also act as an initiating event in lesion formation.

Atherosclerosis develops over the course of many years, and it has been suggested that early pathogenic events, including hypercholesterolemia *in utero*, may influence susceptibility to atherogenesis later in life (30). In the United States, the seroprevalence of HCMV is 60 to 70% between years 40 to 49 of age (2). While it is impossible to know for certain the average age of HCMV acquisition of this population, the current seroprevalence of children under 10 years of age suggests that approximately half of all HCMV-seropositive adults at age 50 initially acquired HCMV in early childhood. It is currently not known how the age of HCMV acquisition might affect lesion formation and progression. It would be interesting to examine the progression of atherosclerotic lesions and immunological responses in individuals infected in early childhood compared to those who are infected much later in life. The results might provide insight into some of the differences that are observed in clinical studies.

Increased susceptibility of ECs to HCMV in atherosclerosis-prone sites might have significant implications for the role of HCMV in pathogenesis of atherosclerosis. Several studies have used normal and hypercholesterolemic mouse models to examine the role of mouse cytomegalovirus (MCMV) infection in atherosclerosis and have documented that MCMV infection accelerates lesion formation (8). Infection of mice with MCMV has also been shown to increase expression of proatherosclerotic genes in the aorta as well as serum levels of interleukin 6 (IL-6), monocyte chemoattractant protein 1 (MCP-1), and tumor necrosis factor alpha (TNF-α) (22). In one study, it was also reported that MCMV infection alone of C57BL/6 wild-type (wt) mice on a normal diet causes an increase in arterial blood pressure (9). Moreover, viral DNA and immediate-early mRNA were found in the aortic root, thoracic aorta carotid artery, and post cava vein at 3 weeks postinfection, and viral DNA could still be detected at 6 weeks postinfection. Only mice that were fed a high-cholesterol diet for 10 weeks as well as infected with MCMV for 6 weeks developed atherosclerotic plaques in the aortas. Neither high cholesterol alone nor MCMV infection alone induced atherosclerosis during this time period.

In addition to the effects on HCMV entry, we have shown that shear stress also modulates HCMV gene expression, production of viral progeny, and spread of the virus. Compared to STAT and HSS, ECs exposed to LSS expressed the highest levels of late viral gene products, produced the highest titers of viral progeny, and spread most efficiently throughout the culture. Taken together, our results suggest that conditions in atheroprone regions of the vascular tree (areas of LSS) promote HCMV lytic infection, which may have a significant impact on pathogenesis *in vivo*. For example, increased production and spread of the virus in these sites might promote dissemination of the virus within the artery wall, promoting further pathophysiological changes in neighboring smooth muscle cells. CMV infection of smooth muscle cells in the artery walls of rodents has been associated with intimal hyperplasia, increased inflammation, and recruitment of lymphocytes in the artery wall (4, 20, 24). In humans, HCMV has been found to be associated with sites of intimal thickening, even in young trauma victims, supporting the hypothesis that HCMV infection may play a role in early atherosclerotic lesions (48).

We also found that regardless of magnitude, exposure of ECs to shear stress increased the kinetics of virion assembly compared to that of ECs exposed to STAT. One possible explanation for the increase is that the cellular environment in ECs exposed to shear stress is more primed to facilitate viral replication than ECs maintained in static conditions. Work by the McIntire group highlights the differences in ECs cultured in flow versus static conditions. Using a whole-genome microarray, they compared global gene expression of human umbilical vein ECs cultured under STAT, LSS, and HSS. Surprisingly, they found that most of the differentially expressed genes (approximately 3,000) were between ECs exposed to STAT and shear stress, regardless of magnitude (13). Differentially expressed genes fell into a number of functional groups, including cytoskeleton, cell cycle, and metabolism, any of which may have an effect on the kinetics of viral assembly and late protein expression. There were much fewer differentially expressed genes between ECs exposed to LSS and those exposed to HSS (approximately 200). Many of these genes fell into functional classes that have been implicated in pathogenesis of atherosclerosis, such as inflammation, matrix metalloproteases, and cell cycle regulation (13). A number of the transcription factors that have

been shown to be differentially regulated in LSS versus HSS have also been implicated in regulation of HCMV gene expression. For example, in cells exposed to LSS, activation of NF-κB and AP-1 promotes expression of proinflammatory and prothrombotic genes, while ECs exposed to HSS activate KLF2 and NRF2 to promote expression of anti-inflammatory and vasoprotective genes (7). During HCMV infection, NF-κB and AP-1 have been suggested to promote viral IE expression (14, 23). NRF2 has been shown to be sequestered to the cytoplasm during infection in fibroblasts, implicating other viral-infection-specific mechanisms to protect the cell from reactive oxygen species (42). Differences in the concentration and/or activation of these transcription factors, cell cycle components, or metabolic intermediates may all contribute to the differences we observed in viral protein expression and viral assembly in different flow conditions. More work will be needed to decipher how differences in the cellular environment of ECs cultured under different flow conditions affect the production of HCMV progeny during acute infection and reactivation.

How might HCMV infection contribute to the induction or progression of atherosclerosis? There are at least five mechanisms that are not mutually exclusive. First, infection of the cell could lead directly to cell death or irreparable damage. Second, the intracellular environment of the endothelial cell could be altered to change its phenotype from atheroprotective to atheroprone. Third, the production of cytokines could either have a local or systemic effect on endothelial cell function. Fourth, the immunological response to HCMV infection either at a localized site in the artery or at distal sites may result in inflammation. Finally, based on very recent studies, it is possible that the CMV-specific T cell has distinct properties that can contribute to endothelial cell dysfunction and vessel damage (44).

Our studies suggest that atheroprone areas of the vessels are significantly more permissive to HCMV infection, while clinical and animal studies indicate that CMV antigen is associated with both early and more advanced atherosclerotic lesions (4, 10, 31, 49). Taken together, these results support the hypothesis that HCMV infection in atheroprone regions promotes pathogenesis of atherosclerosis at the site of lesion formation. Proof of a causative relationship in humans will require the existence of an effective vaccine against HCMV, but given that clinically significant atherosclerosis is a disease of the aged, it may be many years before this question is answered. Use of the flow model system will allow us to further assess how HCMV infection in atheroprone areas affects inflammatory cytokine secretion and leukocyte adhesion. An understanding of the mechanism of induction/acceleration of atherosclerosis by HCMV will be required in order to identify new viral targets and improve interventions for HCMV-related cardiovascular disease.

ACKNOWLEDGMENTS

We thank Marilyn Farquhar for use of the Electron Microscopy Facility and Ying Jones for sample preparation.

This work was supported by Ruth L. Kirschstein National Research Service Award NIH/NCI T32 CA009532 and NIH/NHLBI F32 HL099072 (to J.B.D.). This work was supported by NIH/NCI R01CA034729 and R21AI094180 (to D.H.S.) and NHLBI R01HL106579 (to S.C.).

REFERENCES

1. **Adam E, et al.** 1987. High levels of cytomegalovirus antibody in patients requiring vascular surgery for atherosclerosis. Lancet **ii**:291–293.
2. **Bate SL, Dollard SC, Cannon MJ.** 2010. Cytomegalovirus seroprevalence in the United States: the national health and nutrition examination surveys, 1988–2004. Clin. Infect. Dis. **50**:1439–1447.
3. **Bentz GL, Yurochko AD.** 2008. Human CMV infection of endothelial cells induces an angiogenic response through viral binding to EGF receptor and beta1 and beta3 integrins. Proc. Natl. Acad. Sci. U. S. A. **105**:5531–5536.
4. **Berencsi K, et al.** 1998. Early atherosclerotic plaques in the aorta following cytomegalovirus infection of mice. Cell Adhes. Commun. **5**:39–47.
5. **Blum A, et al.** 1998. High anti-cytomegalovirus (CMV) IgG antibody titer is associated with coronary artery disease and may predict post-coronary balloon angioplasty restenosis. Am. J. Cardiol. **81**:866–868.
6. **Bodaghi B, et al.** 1999. Entry of human cytomegalovirus into retinal pigment epithelial and endothelial cells by endocytosis. Investig. Ophthalmol. Visual Sci. **40**:2598–2607.
7. **Boon RA, Horrevoets AJ.** 2009. Key transcriptional regulators of the vasoprotective effects of shear stress. Hamostaseologie **29**:39–43.
8. **Burnett MS, et al.** 2004. Murine cytomegalovirus infection increases aortic expression of proatherosclerotic genes. Circulation **109**:893–897.
9. **Cheng J, et al.** 2009. Cytomegalovirus infection causes an increase of arterial blood pressure. PLoS Pathog. **5**:e1000427. doi:10.1371/journal.ppat.1000427.
10. **Chiu B, Viira E, Tucker W, Fong IW.** 1997. Chlamydia pneumoniae, cytomegalovirus, and herpes simplex virus in atherosclerosis of the carotid artery. Circulation **96**:2144–2148.
11. **Chiu JJ, Chien S.** 2011. Effects of disturbed flow on vascular endothelium: pathophysiological basis and clinical perspectives. Physiol. Rev. **91**:327–387.
12. **Compton T, Nowlin DM, Cooper NR.** 1993. Initiation of human cytomegalovirus infection requires initial interaction with cell surface heparan sulfate. Virology **193**:834–841.
13. **Conway DE, Williams MR, Eskin SG, McIntire LV.** 2010. Endothelial cell responses to atheroprone flow are driven by two separate flow components: low time-average shear stress and fluid flow reversal. Am. J. Physiol. Heart Circ. Physiol. **298**:H367–H374.
14. **DeMeritt IB, Milford LE, Yurochko AD.** 2004. Activation of the NF-kappaB pathway in human cytomegalovirus-infected cells is necessary for efficient transactivation of the major immediate-early promoter. J. Virol. **78**:4498–4507.
15. **Dumortier J, et al.** 2008. Human cytomegalovirus secretome contains factors that induce angiogenesis and wound healing. J. Virol. **82**:6524–6535.
16. **Feire AL, Koss H, Compton T.** 2004. Cellular integrins function as entry receptors for human cytomegalovirus via a highly conserved disintegrin-like domain. Proc. Natl. Acad. Sci. U. S. A. **101**:15470–15475.
17. **Frangos JA, Eskin SG, McIntire LV, Ives CL.** 1985. Flow effects on prostacyclin production by cultured human endothelial cells. Science **227**:1477–1479.
18. **Gimbrone MA.** 2010. The Gordon Wilson lecture. Understanding vascular endothelium: a pilgrim's progress. Endothelial dysfunction, biomechanical forces and the pathobiology of atherosclerosis. Trans Am. Clin. Climatol. Assoc. **121**:115–127.
19. **Gredmark S, Jonasson L, Van Gosliga D, Ernerudh J, Soderberg-Naucler C.** 2007. Active cytomegalovirus replication in patients with coronary disease. Scand. Cardiovasc. J. **41**:230–234.
20. **Grudzinska MK, et al.** 2010. RCMV increases intimal hyperplasia by inducing inflammation, MCP-1 expression and recruitment of adventitial cells to intima. Herpesviridae **1**:7.
21. **Hendrix MG, Daemen M, Bruggeman CA.** 1991. Cytomegalovirus nucleic acid distribution within the human vascular tree. Am. J. Pathol. **138**:563–567.
22. **Hsich E, et al.** 2001. Cytomegalovirus infection increases development of atherosclerosis in apolipoprotein-E knockout mice. Atherosclerosis **156**:23–28.
23. **Isern E, et al.** 2011. The activator protein 1 binding motifs within the human cytomegalovirus major immediate-early enhancer are functionally redundant and act in a cooperative manner with the NF-{kappa}B sites during acute infection. J. Virol. **85**:1732–1746.
24. **Kloppenburg G, et al.** 2005. Cytomegalovirus aggravates intimal hyperplasia in rats by stimulating smooth muscle cell proliferation. Microbes Infect. **7**:164–170.
25. **Lamon BD, Hajjar DP.** 2008. Inflammation at the molecular interface of atherogenesis: an anthropological journey. Am. J. Pathol. **173**:1253–1264.
26. **Liu R, et al.** 2006. Presence and severity of Chlamydia pneumoniae and

cytomegalovirus infection in coronary plaques are associated with acute coronary syndromes. Int. Heart J. **47**:511–519.
27. **Melnick JL, et al.** 1983. Cytomegalovirus antigen within human arterial smooth muscle cells. Lancet **ii**:644–647.
28. **Merigan TC, et al.** 1992. A controlled trial of ganciclovir to prevent cytomegalovirus disease after heart transplantation. New Engl. J. Med. **326**:1182–1186.
29. **Mocarski ES, Shenk T, Pass RF.** 2007. Cytomegaloviruses, fifth ed, vol 2. Wolters Kluwer Health/Lippincott Williams & Wilkins, Philadelphia, PA.
30. **Napoli C, et al.** 1999. Influence of maternal hypercholesterolaemia during pregnancy on progression of early atherosclerotic lesions in childhood: Fate of Early Lesions in Children (FELIC) study. Lancet **354**:1234–1241.
31. **Pampou S, et al.** 2000. Cytomegalovirus genome and the immediate-early antigen in cells of different layers of human aorta. Virchows Arch. **436**: 539–552.
32. **Raines EW, Ross R.** 1993. Smooth muscle cells and the pathogenesis of the lesions of atherosclerosis. Br. Heart J. **69**:S30–S37.
33. **Reinhardt B, et al.** 2005. HCMV infection of human vascular smooth muscle cells leads to enhanced expression of functionally intact PDGF beta-receptor. Cardiovasc. Res. **67**:151–160.
34. **Ridker PM, Hennekens CH, Buring JE, Kundsin R, Shih J.** 1999. Baseline IgG antibody titers to Chlamydia pneumoniae, Helicobacter pylori, herpes simplex virus, and cytomegalovirus and the risk for cardiovascular disease in women. Ann. Intern. Med. **131**:573–577.
35. **Ross R.** 1999. Atherosclerosis—an inflammatory disease. New Engl. J. Med. **340**:115–126.
36. **Ryckman BJ, Jarvis MA, Drummond DD, Nelson JA, Johnson DC.** 2006. Human cytomegalovirus entry into epithelial and endothelial cells depends on genes UL128 to UL150 and occurs by endocytosis and low-pH fusion. J. Virol. **80**:710–722.
37. **Ryckman BJ, et al.** 2008. Characterization of the human cytomegalovirus gH/gL/UL128-131 complex that mediates entry into epithelial and endothelial cells. J. Virol. **82**:60–70.
38. **Schmolke S, Kern HF, Drescher P, Jahn G, Plachter B.** 1995. The dominant phosphoprotein pp65 (UL83) of human cytomegalovirus is dispensable for growth in cell culture. J. Virol. **69**:5959–5968.
39. **Soroceanu L, Akhavan A, Cobbs CS.** 2008. Platelet-derived growth factor-alpha receptor activation is required for human cytomegalovirus infection. Nature **455**:391–395.
40. **Stinski MF, Petrik DT.** 2008. Functional roles of the human cytomegalovirus essential IE86 protein. Curr. Top. Microbiol. Immunol. **325**:133–152.
41. **Streblow DN, et al.** 1999. The human cytomegalovirus chemokine receptor US28 mediates vascular smooth muscle cell migration. Cell **99**:511–520.
42. **Tilton C, Clippinger AJ, Maguire T, Alwine JC.** 2011. Human cytomegalovirus induces multiple means to combat reactive oxygen species. J. Virol. **85**:12585–12593.
43. **Valantine HA, et al.** 1999. Impact of prophylactic immediate post-transplant ganciclovir on development of transplant atherosclerosis: a post hoc analysis of a randomized, placebo-controlled study. Circulation **100**:61–66.
44. **van de Berg PJ, Yong SL, Remmerswaal EB, van Lier RA, ten Berge IJ.** 2012. Cytomegalovirus-induced effector T cells cause endothelial cell damage. Clin. Vaccine Immunol. **19**:772–779.
45. **Vliegen I, Stassen F, Grauls G, Blok R, Bruggeman C.** 2002. MCMV infection increases early T-lymphocyte influx in atherosclerotic lesions in *apoE* knockout mice. J. Clin. Virol. **25**(Suppl 2):S159–S171.
46. **Wang X, Huang DY, Huong SM, Huang ES.** 2005. Integrin alphavbeta3 is a coreceptor for human cytomegalovirus. Nat. Med. **11**:515–521.
47. **Wang X, Huong SM, Chiu ML, Raab-Traub N, Huang ES.** 2003. Epidermal growth factor receptor is a cellular receptor for human cytomegalovirus. Nature **424**:456–461.
48. **Yamashiroya HM, Ghosh L, Yang R, Robertson AL, Jr.** 1988. Herpesviridae in the coronary arteries and aorta of young trauma victims. Am. J. Pathol. **130**:71–79.
49. **Yi L, Wang DX, Feng ZJ.** 2008. Detection of human cytomegalovirus in atherosclerotic carotid arteries in humans. J. Formosan Med. Assoc. **107**: 774–781.